Quantitative 3D imaging of scattering media using structured illumination and computed tomography

Kristensson, Elias; Berrocal, Edouard; Aldén, Marcus

Published in:
Optics Express

DOI:
10.1364/OE.20.014437

2012

Document Version:
Publisher's PDF, also known as Version of record

Quantitative 3D imaging of scattering media using structured illumination and computed tomography

E. Kristensson,* E. Berrocal, and M. Aldén

Division of Combustion Physics, Lund Institute of Technology, Box 118, S-221 00 Lund University, Sweden

*elias.kristensson@forbrf.lth.se

Abstract: An imaging technique capable of measuring the extinction coefficient in 3D is presented and demonstrated on various scattering media. The approach is able to suppress unwanted effects due to both multiple scattering and light extinction, which, in turbid situations, seriously hampers the performance of conventional imaging techniques. The main concept consists in illuminating the sample of interest with a light source that is spatially modulated in both the vertical and horizontal direction and to measure, using Structured Illumination, the correct transmission in 2D at several viewing angles. The sample is then reconstructed in 3D by means of a standard Computed Tomography algorithm. To create the adequate illumination, a novel "crossed" structured illumination approach is implemented. In this article, the accuracy and limitation of the method is first evaluated by probing several homogeneous milk solutions at various levels of turbidity. The unique possibility of visualizing an object hidden within such solutions is also demonstrated. Finally the method is applied on two different inhomogeneous scattering spray systems; one transient and one quasi-steady state.

OCIS codes: (290.4210) Multiple scattering; (290.7050) Turbid media; (110.0113) Imaging through turbid media; (290.2200) Extinction; (110.6955) Tomographic imaging.

References and links

1. M. Padgett, "Penetrating scattering media," Nat. Photonics **4**, 741–742 (2010).
2. M. Linne, M. Paciaroni, E. Berrocal, and D. Sedarsky, "Ballistic imaging of liquid breakup processes in dense sprays," in Proceedings of the Combustion Institute (2009), Vol. 32, pp. 2147–2161.
3. O. S. Ugolnikov, O. V. Postylyakov, and I. A. Maslova, "Effects of multiple scattering and atmospheric aerosol on the polarization of the twilight sky," J. Quant. Spectrosc. Radiat. Transfer **88**, 233–241 (2004).
4. S. G. Narasimhan, S. K. Nayar, B. Sun, and S. J. Koppal, "Structured light in scattering media," in Proceedings of the Tenth IEEE International Conference on Computer Vision (2005).
5. G. Zaccanti, P. Bruscaglioni, M. Gurioli, and P. Sansoni, "Laboratory simulations of lidar returns from clouds: experimental and numerical results," Appl. Opt. **32**, 1590–1597 (1993).
6. W.-F. Cheong, S. A. Prahl, and A. J. Welch, "A review of the optical properties of biological tissues," IEEE J. Quant. Electron. **26**, 2166–2185 (1990).
7. T. Breuninger, K. Greger, and E. H. K. Stelzer, "Lateral modulation boosts image quality in single plane illumination fluorescence microscopy," Opt. Lett. **32**, 1938–1940 (2007).
8. E. Berrocal, E. Kristensson, M. Richter, M. Linne, and M. Aldén, "Application of structured illumination for multiple scattering suppression in planar laser imaging of dense sprays," Opt. Express **16**, 17870–17881 (2008).
9. R. Wellander, E. Berrocal, E. Kristensson, M. Richter, and M. Aldén, "Three-dimensional measurement of the local extinction coefficient in a dense spray," Meas. Sci. Technol. **22**, 855–861 (2011).

#162357 - $15.00 USD Received 1 Feb 2012; revised 29 Mar 2012; accepted 11 Apr 2012; published 13 Jun 2012

10. C. F. Powell, Y. Yue, R. Poolab, and J. Wanga, "Time-resolved measurements of supersonic fuel sprays using synchrotron x-rays," J. Synchrotron Radiat. **7**, 356–360 (2000).
11. W. Cai, C. F. Powell, Y. Yue, S. Narayanan, J. Wanga, M. W. Tate, M. J. Renzi, A. Ercan, E. Fontes, and S. M. Grunere, "Quantitative analysis of highly transient fuel sprays by time-resolved x-radiography," Appl. Phys. Lett. **83**, 1671–1673 (2003).
12. A. Kak and M. Slaney, *Principles of Computerized Tomographic Imaging* (Academic Press, 1999).
13. M. A. A. Neil, R. Juškaitis, and T. Wilson, "Method of obtaining optical sectioning by using structured light in a conventional microscope," Opt. Lett. **22**, 1905–1907 (1997).
14. Q. Wu, F. A. Merchant, and K. R. Castleman, *Microscope Image Processing* (Academic Press, 2008).
15. D. J. Cuccia, F. Bevilacqua, A. J. Durkin, and B. J. Tromberg, "Modulated imaging: quantitative analysis and tomography of turbid media in the spatial-frequency domain," Opt. Lett. **30**, 1354–1356 (2005).
16. J. Chen, V. Venugopal, F. Lesage, and X. Intes, "Time-resolved diffuse optical tomography with patterned-light illumination and detection," Opt. Lett. **35**, 2121–2123 (2010).
17. N. Ducros, A. Bassi, G. Valentini, M. Schweiger, S. Arridge, and C. D'Andrea, "Muliple-view fluorescence optical tomography reconstruction using compression of experimental data," Opt. Lett. **36**, 1377–1379 (2011).
18. W. Choi, C. Fang-Yen, K. Badizadegan, S. Oh, N. Lue, R. R. Dasari, and M. S. Feld, "Tomographic phase microscopy," Nat. Methods **4**, 717–719 (2007).
19. E. Berrocal, D. L. Sedarsky, M. E. Paciaroni, I. V. Meglinski, and M. A. Linne, "Laser light scattering in turbid media. Part I: Experimental and simulated results for the spatial intensity distribution," Opt. Express **15**, 10649–10665 (2007).
20. E. Kristensson, L. Araneo, E. Berrocal, J. Manin, M. Richter, M. Aldén, and M. Linne, "Analysis of multiple scattering suppression using structured laser illumination planar imaging in scattering and fluorescing media," Opt. Express **19**, 13674–13663 (2011).

1. Introduction

The analysis and imaging of scattering media is of large interest in a variety of fields such as microscopy [1], combustion engineering [2], atmospheric monitoring [3] as well as for solving visibility issues within foggy environments or turbid water [4]. One special characteristic of scattering media is their dimensionless nature; for instance, as long as the number of scattering events is equal, the light scattered by a cloud in the sky can be experimentally simulated at a centimeter scale in a laboratory [5]. In addition to scattering, radiation can also be absorbed while propagating through a turbid medium. Vast experimental campaigns have focused on measuring the scattering and absorption cross-section of human tissue [6]. In the literature, the total loss of light induced by these two phenomena is referred to as *extinction*. The present article demonstrates a novel approach to determine the extinction of light, spatially resolved in three dimensions.

Despite being randomly inhomogeneous at a molecular scale, scattering media can, at a macroscopic scale, also be defined as either homogeneous (e.g. turbid solutions, milk, fog, pharmaceutical tablets) or inhomogeneous (e.g. tissue layers, embryos, spray systems). Single point measurements usually provide satisfactory results when applied on homogeneous samples. However, in the case of inhomogeneous media, where the sample exhibits gradients and variations of the extinction coefficient, 2D or, if possible, 3D imaging is required. High pressure, atomizing fuel sprays are typical examples of highly inhomogeneous macroscopic scattering media. Such sprays produce an ensemble of fine polydisperse droplets which disperse in the surrounding air as they travel away from the nozzle tip. These systems are widely used in diesel and gas turbine engines to disintegrate the liquid fuel into a combustible air/fuel mixture. The need for detailed characterization of fuel sprays is of great importance as it governs both the efficiency of the combustion as well as the emission of pollutants. However, quantitative imaging of atomizing sprays by means of visible light is particularly challenging, mostly due to errors associated with multiple light scattering.

Recently a laser sheet-based imaging technique capable of reducing errors induced by multiple scattering was demonstrated, in the field of microscopy by Breuninger *et al.* [7] and for spray imaging by Berrocal *et al.* [8]. The method, named Structured Laser Illumination Planar

#162357 - $15.00 USD Received 1 Feb 2012; revised 29 Mar 2012; accepted 11 Apr 2012; published 13 Jun 2012

Imaging (SLIPI) [8], differentiates between singly and multiply scattered light by modulating the intensity profile of the incident laser sheet. A photon that undergoes several scattering events loses this structural information, in contrast to a singly scattered photon.

Reducing the amount of multiply scattered light being detected leads to higher image contrast, however, light-extinction still remains an issue. Recently, Wellander *et al*. presented a scanning approach to correct for extinction [9]. This method is based on performing several SLIPI measurements at different locations within a spray and, for each location, to measure the path-integrated attenuation of light. Another way to avoid multiple light scattering is to use X-rays instead of visible light. In this case, scattering becomes negligible, allowing the spray to be characterized by measuring line-of-sight absorption [10]. However, it should be noted that to obtain measurable levels of absorption it is often required to add absorbers to the injected liquid. With careful calibration, this approach provides means to accurately measure the extinction of light through optically dense sprays, which, in turn, can be used for tomographic imaging [11].

In this article we present an alternative method to quantitatively image inhomogeneous turbid media in 3D using visible light instead of X-rays. The approach is based on measuring the path-integrated extinction of light in two dimensions at several viewing angles. This allows the local extinction coefficient to be calculated in 3D by means of standard CT algorithms. However, since these algorithms are based on the Beer-Lambert law, it is imperative to suppress both the scattered- and multiply scattered light intensity contribution. Failure in removing this extraneous light can lead to large errors and uncertainties in the sample reconstruction process, an issue which is solved here by implementing structured illumination (SI). The proposed method is first tested on various controlled scattering environments consisting of homogeneous milk solutions at different levels of dilution. The possibility of visualizing an object placed in such media is also demonstrated. Finally, the capabilities of the technique is demonstrated on a transient gasoline direct injection (GDI) spray and on a multi-hole aerated water spray.

2. Theory

2.1. Computed tomography

Since its invention, transmission computed tomography, which is a quantitative imaging technique, has played an important role for medical diagnostics. The basic principle consists in measuring the path-integrated attenuation of light intensity through an object, commonly using a sheet of X-ray light. This process is repeated for different viewing angles by rotating either the object or the light source together with the detection system. The acquired set of data, usually referred to as a sinogram, bears information about the spatial distribution of the attenuators. Extracting this information and thereby reconstructing the sample, either in 2D or in 3D, is the aim of computed tomography. Achieving this end can be accomplished through various algorithmic means; back projection, filtered-back projection, Fourier reconstruction and iterative techniques [12]. For the measurements presented within this article the second approach is implemented.

Figure 1 shows an example of CT based on 1D transmission data of the so-called Shepp and Logan “head phantom”. The sample is rotated and for each viewing angle a transmission measurement, presented in the graphs, is performed. By stacking these results a 2D representation, the sinogram, of the acquired data set is obtained. In the example given in Fig. 1 the sinogram is built up by 180 viewing angles. Also illustrated in the example is the difference between back projection and filtered-back projection. In principle, these approaches rebuilds the sample by “smearing” each 1D transmission view back through an image matrix along the direction it was originally acquired. The final image is formed by taking the sum of all the back-projected views. Having few viewing angles leads to a low quality reconstruction to-

#162357 - $15.00 USD Received 1 Feb 2012; revised 29 Mar 2012; accepted 11 Apr 2012; published 13 Jun 2012

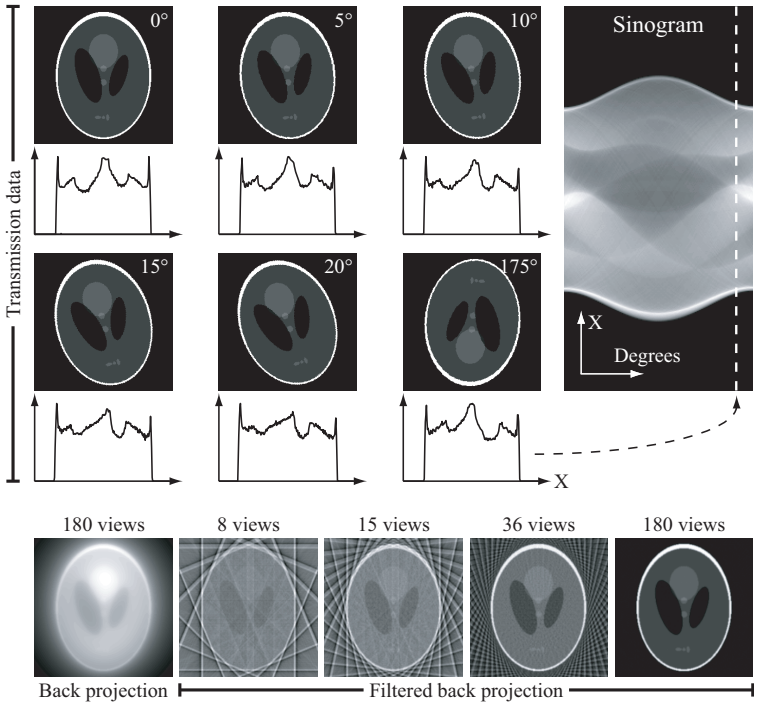

Fig. 1. Illustration of computed tomography, showing the sample at six different viewing angles together with the corresponding transmission data. A 2D representation of the data set is also shown (sinogram). Reconstruction based on back projection leads to significant blurring which is avoided by applying a frequency filter on the transmission data (filtered-back projection).

gether with image artefacts, as seen in Fig. 1. Also noticeable is that ordinary back filtering gives rise to blurring, which is avoided by frequency filtering the transmission data, hence the name filtered-back projection.

Regardless of the algorithm used to rebuild the sample the accuracy and resolution of the final reconstructed image depends mainly on two aspects; the number of viewing angles and the fidelity of the transmission measurement. The current investigation aims at improving the second aspect, where we focus our attention on 2D measurements performed on turbid scattering media with visible light sources. In this case, photons which have been scattered while propagating through the medium may be detected and the sample falsely appears to be less opaque, which, in turn, leads to an underestimation of the desired optical quantity. In addition, the resulting shadow created by the sample lose image contrast because of this contribution of light which also can cause errors in the reconstruction. The current study aims at investigating whether these unwanted effects can be reduced by means of structured illumination.

2.2. Structured illumination

Structured illumination (SI) is an imaging technique developed in 1997 by Neil *et al.* within the field of microscopy [13]. The main purpose of the technique is to reduce out-of-focus light that degrades the depth-resolution and thereby also the image contrast. It became popular because of its relatively simple experimental setup and that it provides optically sectioned images with very few exposures, unlike previous solutions such as confocal microscopy that requires a scanning

#162357 - $15.00 USD Received 1 Feb 2012; revised 29 Mar 2012; accepted 11 Apr 2012; published 13 Jun 2012

process [14]. The principle of SI is to take advantage of the fact that image details are only sharp if they originate from the in-focus plane, while remaining parts of the sample appears blurry. This is also the case for the illumination. Therefore, by superimposing a structure onto the incident light it is possible to differentiate between light originating from the in-focus plane and the out-of-focus intensity. For SI, the sample is normally illuminated with a sinusoidal intensity grid pattern. Suppression of the out-of-focus light is performed *after* the image acquisition and the process requires at least three recordings, between which the spatial phase of the sinusoidal intensity modulation is shifted $2\pi/3$. This change in phase is not seen in the blurry out-of-focus light; its intensity contribution remains constant in the three frames. It can be shown that by extracting the pair-wise difference between the acquisitions, according to Eq. (1), the in-focus information is retained while the undesired out-of-focus light is suppressed [13].

$$I_S(x,y) = \frac{\sqrt{2}}{3} \cdot \sqrt{(I_0 - I_{2\pi/3})^2 + (I_0 - I_{4\pi/3})^2 + (I_{2\pi/3} - I_{4\pi/3})^2} \tag{1}$$

Here I_S denotes the final depth-resolved image and I_X is one of the three recordings where the subscript X indicates the phase of the incident modulation. Another advantage with SI is the possibility of extracting the "conventional" image I_C from the same set of data (see Eq. (2)). I_C is (in theory) equal to the image one would obtain if an ordinary non-modulated illumination scheme was applied. This allows the results from the two different techniques to be compared and improvements in image quality to be quantified. Note that image differences between I_C and the non-modulated case may exist, for instance if the signal response is non-linear or if the phases of the modulated images are erroneous.

$$I_C(x,y) = \frac{I_0 + I_{2\pi/3} + I_{4\pi/3}}{3} \tag{2}$$

The filtering capabilities of SI can be advantageous for transmission imaging as well. However, in contrast to the original purpose of the technique, depth-resolution is not desired for the present investigation as computed tomography relies on line-of-sight data. Adapting SI for transmission imaging can be achieved by guiding a 2D light beam, intensity modulated in one direction, through the sample of interest and onto a screen, which then is imaged. Photons that were scattered, either once or several times, while propagating through the sample may still be detected but will not carry the encoded structural information (these can be considered to have the same characteristics as out-of-focus light). SI-transmission data can be extracted by performing two additional recordings between which the incident modulation pattern is shifted $2\pi/3$ (as is required for SI). Processing the data according to Eq. (1) will suppress scattered light, resulting in an image mostly consisting of the unperturbed light.

In an attempt to improve the selectivity and accuracy of SI a slightly more sophisticated illumination scheme is employed for the measurements presented in this article. Instead of modulating the incident beam in one direction only, the beam intensity profile is modulated in both the vertical direction as well as in the horizontal direction. This approach, which we call "crossed"-SLITI (crossed-Structured Laser Illumination Transmission Imaging), has shown to reduce the presence of image artefacts (residual line structures) that generally is an issue with SI which, in effect, will render errors in the CT reconstruction. The drawback with this method is that three images must be recorded at each of the three spatial phases of the horizontal intensity modulation (one image for each vertical spatial phase), resulting in a total of nine images. The final SI-transmission image is calculated according to

$$I_S(x,y) = \frac{\sqrt{2}}{9} \cdot \sqrt{\sum_{i=1}^{8} \sum_{k=i+1}^{9} (I_i - I_k)^2} \tag{3}$$

#162357 - $15.00 USD Received 1 Feb 2012; revised 29 Mar 2012; accepted 11 Apr 2012; published 13 Jun 2012

where the subscripts denote the different raw data images, each having a different combination of horizontal and vertical spatial phases.

2.3. Combining CT and SI

The concept of combining structured illumination and computed tomography is not completely new. Cuccia *et al.* illuminated a turbid medium with different spatial frequencies superimposed on the incident light and took advantage of the fact that lower frequencies penetrate farther into the sample compared to higher ones. This allows different depths to be probed, which, in turn, can be used to create a 3D reconstruction of the medium, without being required to rotate the sample [15]. Other approaches for diffuse optical tomography can be found in the literature, for instance by combining time-gating and patterned-light illumination [16] or by means of multiple-view fluorescence detection [17]. Choi *et al.* combined SI and CT to measure the index of refraction in 3D by utilizing a phase-shifting laser interferometer. Three-dimensional information was obtained by varying the illumination angle, i.e. following the concept of tomographic imaging described in this chapter. This approach is, however, only suitable for dilute media [18].

Unlike these previously published approaches, the current method employs SI to visualize the path-integrated attenuation of light (in 2D) through a turbid scattering medium at several different viewing angles. The data is then analyzed using a filtered-back projection algorithm, which, in turn, allows the extinction coefficient to be reconstructed in 3D.

3. Experimental arrangement

A sinusoidal intensity pattern can be created with a coherent light source in several ways. The most straightforward approach is to illuminate a sinusoidal grid target and to form an image of this onto the sample. However, this will only render a sharp pattern at the image plane and is therefore not perfectly suited for line-of-sight transmission imaging. An alternative approach is to illuminate a square grid pattern and to spatially filter out all but the ± 1 interference orders, thus creating two identically intense coherent light sources. By letting these beams interfere they will create the desired sinusoidal intensity modulation. The main benefit with this method, which is the one employed within the current investigation, is that the modulation strength remains nearly constant with distance. Its main drawback is the loss of light associated with the spatial filtering, making it less suited for low signal applications.

Figure 2 shows a schematic of the optical arrangement used throughout the current study. Two pulsed Nd:YAG lasers (pulse length $\sim$10 ns) each illuminate a Ronchi (square wave, 5 lp/mm) grating, rotated 90 degrees relative each other. The pulses, which are separated $\sim$100 ns in time, are then spatially overlapped using a beam-splitter cube and guided through the frequency filter. With distance, the remaining ± 1 interference orders eventually overlap and interfere, thus creating a sinusoidal modulation, either horizontally (first pulse) or vertically (second pulse). The light is sent through the spray, which is placed on a rotational stage, and then onto a screen which is imaged. By setting the acquisition time adequately long the camera (14 bit iXon-897 EM-CCD, 512×512 pixels) will record the sum of the intensities. The resulting "dotted" pattern can be seen in Fig. 2 (c).

The samples were probed every 5 degrees resulting in a total of 36 viewing angles, which was considered a good trade-off between acquisition time and reconstruction quality (see example in Fig. 1) in order to demonstrate the concept of the approach. However, to minimize image artefacts an increased number of viewing angles is advised. To handle the large amount of data, the pixels were binned either 3×3 or 4×4 (depending on the field-of-view) before being processed with the filtered-back projection algorithm. Ideally for CT measurements, the incoming radiation should not diverge. This requirement cannot be met when implementing SI since the

#162357 - $15.00 USD Received 1 Feb 2012; revised 29 Mar 2012; accepted 11 Apr 2012; published 13 Jun 2012

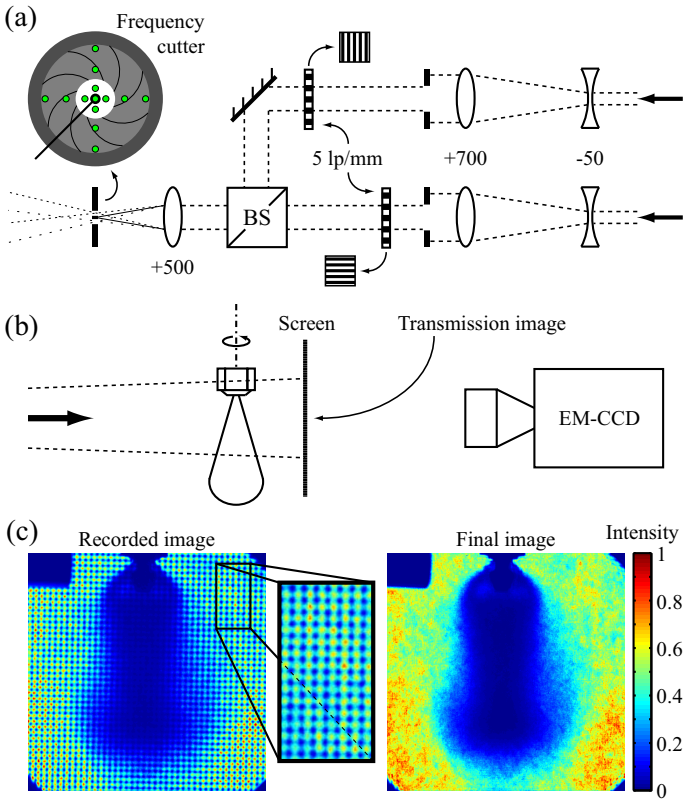

Fig. 2. (a) Optical arrangement for crossed-SLITI. Two laser pulses are each sent through a Ronchi grating, after which the beams are spatially overlapped. Their undesired frequency components are then filtered out (frequency cutter). (b) The structured light source is guided through the spray, which is mounted on a rotational stage. The transmitted light is then imaged as it falls onto a screen. (c) An example of a single modulated transmission image with the corresponding SI-image. The dark part in the top left corner is used as a reference to evaluate the unavoidable camera noise level.

fringe (or dotted) pattern is created through interference. It could be mentioned that there are standard CT algorithms designed to handle a diverging beam arrangement, but such a fan beam illumination differs slightly from the SI approach. The divergence of the beams was for this reason set to a minimum ($\sim$1.5 degrees) to be as near a parallel beam arrangement as possible. By computer simulating the chosen optical scheme it could be deduced that this would not cause any significant errors in the sample reconstruction.

As previously mentioned, the crossed-SLITI approach requires the modulation to be shifted both vertically and horizontally. This is achieved by tilting two glass plates - one for each direction of the modulation - which are situated after the frequency cutter (not shown in Fig. 2). Attempting to use a single laser source in combination with a crossed square target to create the dotted pattern would not suffice and would lead to residual line structures in I_S. This is illustrated in Fig. 3, showing the Fourier transform of a single modulated image together with the Fourier transform of its corresponding I_S image. In the top row the SI pattern was created with a single laser beam guided through a crossed Ronchi pattern, while in the bottom row the SI pattern was achieved using two lasers and two individual Ronchi gratings. Each bright dot in

#162357 - $15.00 USD Received 1 Feb 2012; revised 29 Mar 2012; accepted 11 Apr 2012; published 13 Jun 2012

the figures indicates the presence of a strong sinusoidal component. Ideally, the final I_S image should contain no such sinusoidal components (apart from the one situated in the center, which is the overall mean intensity value), as this would indicate the presence of residual lines. Such image artefacts are not uncommon for structured illumination but are highly undesired. The second approach, with two combined laser beams, shows no residual lines, in contrast to the single beam method.

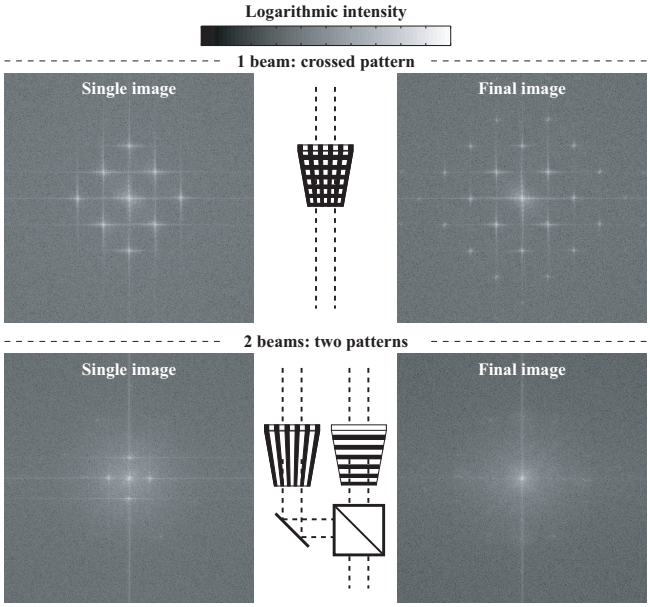

Fig. 3. Two dimensional Fourier transform of one of the nine raw data images and the final structured illumination image (logarithmic intensity scale). *Top row*: Two Ronchi gratings oriented 90 degrees relative each other illuminated with one beam of light. *Bottom row*: Two beams, each (before recombination) illuminating an individual Ronchi grating.

4. Verification

Before applying the crossed-SLITI approach its performance was investigated to determine whether it is suitable for CT measurements. The main aspect under consideration here is the response of the system, accurate quantitative results can only be acquired if the detected signal decrease according to the Beer-Lambert law:

$$I_T = I_0 \cdot e^{-\sigma_e \cdot C \cdot L} = I_0 \cdot e^{-\mu_e \cdot L} = I_0 \cdot e^{-OD} \tag{4}$$

wherein I_T and I_0 is the transmitted and initial intensity, respectively, σ_e is the average extinction cross-section (mm^2) over a distance L (mm), μ_e is the average extinction coefficient (mm^{-1}) over the same length, C is the concentration of attenuating particles (mm^{-3}) and OD is the optical depth. One straightforward approach to investigate the response is to probe homogenous samples with different values of C (but keeping σ_e and L constant). Ideally in such a case, the ratio I_T/I_0 should decrease exponentially as C increases. Figure 4 shows the result for such measurements for both conventional transmission imaging and crossed-SLITI, where the transmitted light through a cuvette (dimension $10\times10\times30$ mm^3) containing a homogeneous mixture of water and milk was imaged. The concentration of scattering particles was altered

#162357 - $15.00 USD Received 1 Feb 2012; revised 29 Mar 2012; accepted 11 Apr 2012; published 13 Jun 2012

through dilution and each of the 11 measurement points was repeated six times. An average value of I_T and I_0, in which the cuvette only contained water, was then extracted from the 2D transmission images. The left graph in Fig. 4 shows the ratio I_T/I_0 together with an exponential fit. The right graph plots $-\ln(I_T/I_0)$, i.e. an estimation of optical depth, which should increase linearly with C. A linear fit for both curves is included here. As seen, the conventional data points shows a nonlinear trend and a second order polynomial fit seams to capture the shape of the curve more accurately.

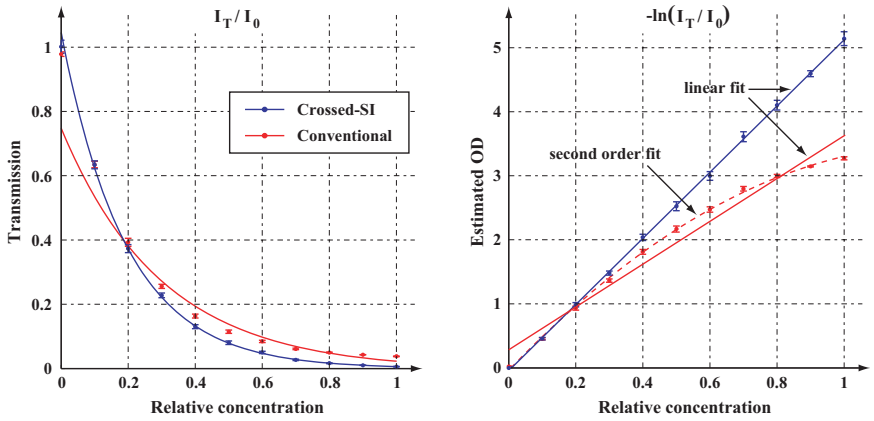

Fig. 4. *Left graph*: The ratio I_T/I_0 as a function of C (relative concentration). The SI approach gives rise to a single exponential decay. *Right graph*: Estimation of optical depth as a function of C. In contrast to the SI results, which increase linearly with C, the conventional results tends to follow a second order polynomial. The error bars indicate the standard deviation.

The two graphs in Fig. 4 illustrate the quantitative differences between conventional transmission imaging and structured illumination. At low concentrations the transmitted intensity for the two imaging techniques coincides and decreases exponentially as C increases, as expected. However, as the OD exceeds unity (estimated from Fig. 4) the results starts to diverge and the conventional signal no longer follows the Beer-Lambert law. Interestingly, this value represents the limit of the single scattering regime ($OD < 1$) [19]. Laser-based techniques are mostly unaffected by errors introduced by multiple scattering when applied on an optically dilute medium (where the average number of scattering events is below one), as is illustrated in this example. These results demonstrate the potential of exceeding this limit for transmission imaging by the implementation of structured illumination. However, even though the estimated OD promisingly increases linearly with relative concentration when applying crossed-SLITI the degree of accuracy still remains uncertain - the linearity does not guarantee accuracy in absolute numbers. Probing a sample containing larger particles may give rise to a reduce accuracy, because the probability for forward scattering is high. In such a case, the initial incident direction of a scattered photon is unaltered and structured illumination cannot differentiate between this contribution and the unperturbed light intensity, as demonstrated by Kristensson *et al.* [20]. This leads to an underestimation of the extinction coefficient μ_e and thereby also the optical depth, yet I_T may still decrease exponentially with concentration (but with a reduced slope). Another uncertainty, mostly associated with spray measurements, concerns the interaction between light and liquid ligaments, as the reduction in intensity in such a case cannot be described by the Beer-Lambert law.

To also demonstrate qualitative differences between conventional transmission imaging and

#162357 - $15.00 USD Received 1 Feb 2012; revised 29 Mar 2012; accepted 11 Apr 2012; published 13 Jun 2012

crossed-SLITI, a second measurement was performed. In this case, a solid object was inserted into a cuvette containing a homogeneous mixture of water and milk (turbidity unknown) and an image of the transmitted light recorded. As can be seen in Fig. 5, without suppressing scattered and multiply scattered light which blurs and conceals image details, the object is almost fully hidden and, consequently, tomographic imaging would not be applicable. In contrast, when applying crossed-SLITI the object is completely visible and even appears to be surrounded by a weak, but clearly noticeable, line. This is believed to arise from diffraction, however, this needs to be verified. Being able to measure diffraction and interference in turbid media is of great interest and can be used for particle sizing, for example. However, for tomographic imaging such patterns are undesired and can, depending on their magnitudes, render errors in the 3D reconstruction. In the current proof-of-principle investigation this effect (and its consequences) is not studied further as diffraction can be avoided through the use of an incoherent light source.

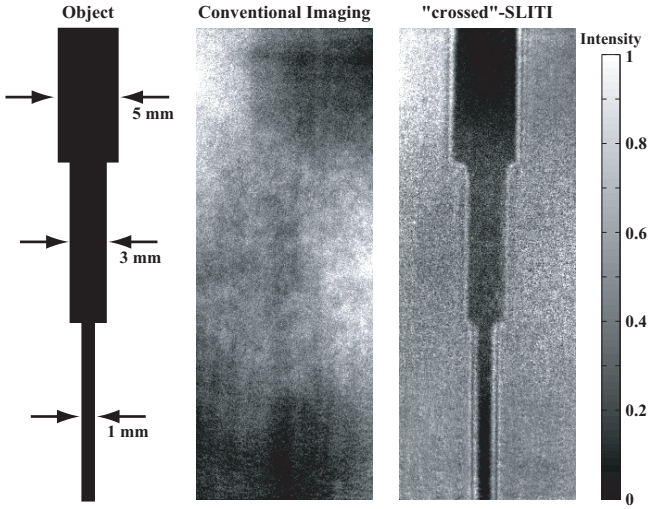

Fig. 5. Qualitative differences in image contrast between conventional transmission imaging and structured illumination. The images show the transmitted light through a cuvette with a homogeneous solution of water and milk wherein a solid object was inserted. Scattered light, which is not suppressed in the conventional case, blurs and conceals the object.

5. Results

The results when applying the crossed-SLITI tomographic approach on two different air-assisted atomizing spray systems are presented in Fig. 6 (6-hole water spray) and in Fig. 7 (transient GDI spray). The results show both the reconstructed 3D images as well as 2D cross-sections, both clearly demonstrating the advantages of the approach. For instance, any skewness in the images caused by extinction, which ordinarily limits imaging of dense media, is avoided. In addition, the implementation of SI prevents the usual loss of image contrast arising due to the detection of multiply scattered light. Apart from avoiding extinction of light and multiple scattering issues, one of the main benefits with the presented approach is that it measures a physical quantity that is directly related to the sample itself. Hence, there is no need to add any dye or tracer compounds, which makes it easier to compare different measurements. The method is, in principle, applicable on any spray system, at least in regions where the *OD* does not exceed $\sim$6 (neglecting practical limitations, e.g. optical access). This upper limit in turbidity is linked with the limited dynamic range of the camera system.

#162357 - $15.00 USD Received 1 Feb 2012; revised 29 Mar 2012; accepted 11 Apr 2012; published 13 Jun 2012

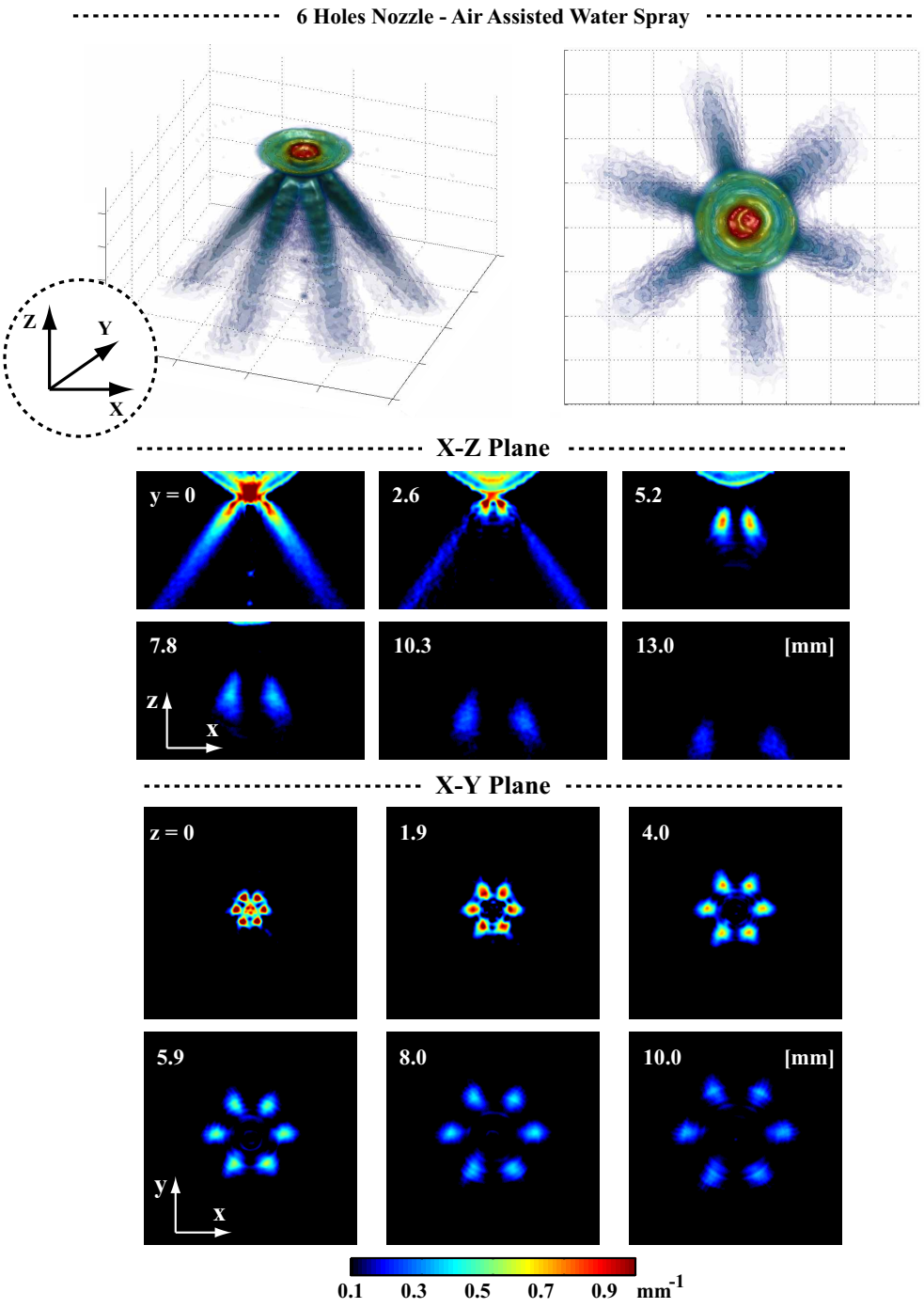

Fig. 6. 3D and 2D images of the 6-hole water spray, obtained using crossed-SLITI tomography. The numbers in the 2D sections indicate the location of the section (origin at nozzle outlet). Notice for instance how the six isolated spray plumes are clearly resolved even near the injector.

#162357 - $15.00 USD Received 1 Feb 2012; revised 29 Mar 2012; accepted 11 Apr 2012; published 13 Jun 2012

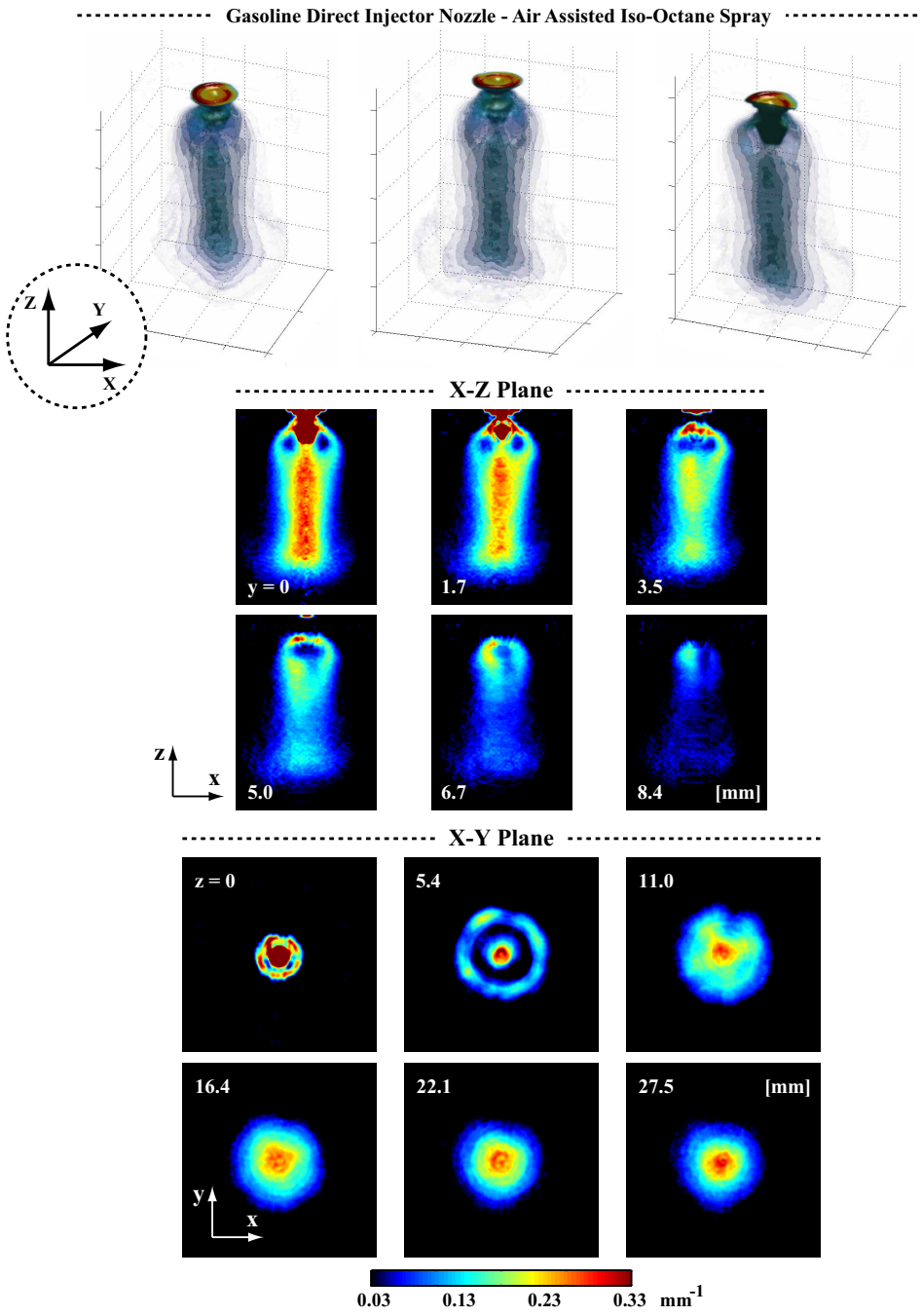

Fig. 7. 3D and 2D images of the transient GDI spray, obtained using crossed-SLITI tomography. Note that only half the spray is shown in the rightmost 3D rendition. The numbers in the 2D sections indicate the location of the section (origin at nozzle outlet). Notice how the hollow region just below the nozzle tip is clearly visible.

#162357 - $15.00 USD Received 1 Feb 2012; revised 29 Mar 2012; accepted 11 Apr 2012; published 13 Jun 2012

It is important to note that liquid ligaments are expected near the orifice of the nozzle. The reduction of light intensity through such volumes may deviate from the Beer-Lambert law and one should therefore be careful when analyzing the data in this region.

There are a variety parameters one needs to consider when performing CT measurements in order to avoid reconstruction errors. First, it is important to keep the sample fluctuations at a minimum. Naturally, due to their stochastic nature, fluctuations are unavoidable when sprays are probed and these must be averaged out. Second, the number of viewing angles should be as high as possible (see example in Fig. 1). The rotation itself is another issue, the sample must be rotated around its central axis and vertical and horizontal displacements are essential to avoid. The turbidity of the sample is also affecting the result. An optical depth exceeding $\sim$6 (depending on the magnitude of the scattered light) would not be possible to measure due to the limited dynamic range of the detection system. Such a case would lead to an underestimation of the extinction coefficient. However, despite all these potential sources of error, the resulting 3D images shows only few signs of artefacts. To inspect the validity of the reconstruction, the results can be compared with the actual measurements. Such a comparison is presented in Fig. 8. The top left image shows one of the 36 *OD* measurements of the 6-hole water spray whereas the top right image is a 2D map of *OD* calculated from the 3D reconstruction data. Ideally these two images should be identical. The two graphs show a detailed comparison along the dashed lines in the top left image and although some discrepancies can be noticed, the computer model performs well in reconstructing the probed volume.

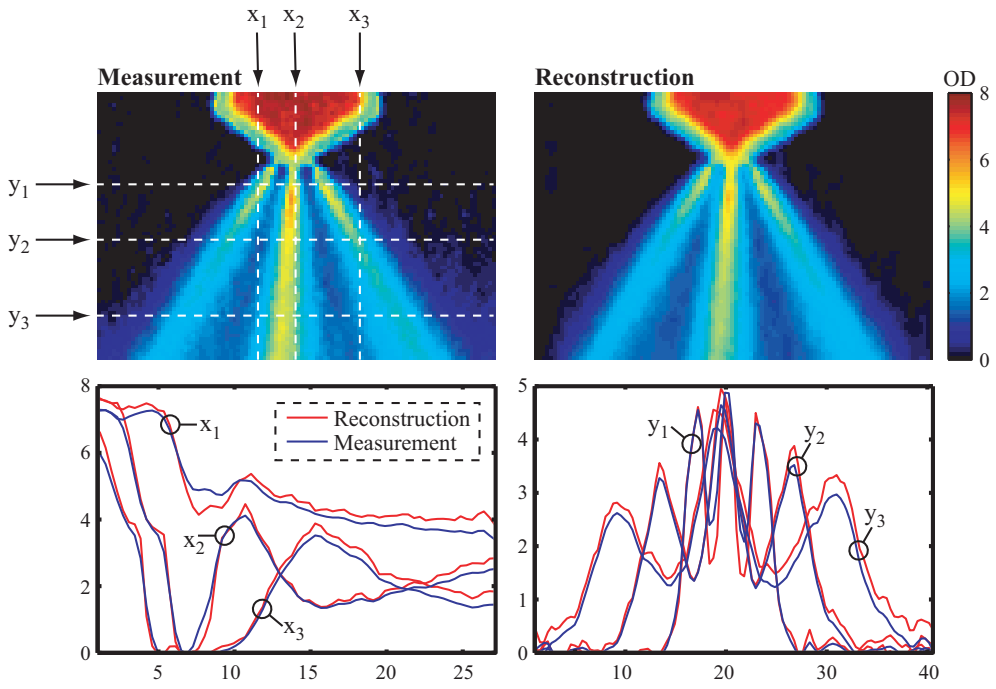

Fig. 8. Comparison between the acquired *OD* data (top left image) and an "artificial" *OD* map extracted from the reconstructed 3D data (top right image). The graphs shows cross sections (see dashed lines) of the *OD* values from both images.

#162357 - $15.00 USD Received 1 Feb 2012; revised 29 Mar 2012; accepted 11 Apr 2012; published 13 Jun 2012

6. Conclusion

A diagnostic tool for three-dimensional imaging of the extinction coefficient suitable for measurements of relatively dense, scattering media has been demonstrated. The technique is based on a combination of two-dimensional transmission imaging and computed tomography to provide quantitative data in 3D. Implementing structured illumination strongly reduces the scattered light intensity, which is essential for accurate transmission measurements. The response of the technique has been investigated and provides satisfying results up to an estimated optical depth of $\sim$6, whereas 2D transmission measurements without suppression of scattered light show discrepancies already at $OD > 1$. Further investigations are, however, needed to determine the accuracy of the results when relatively large spherical particles (with respect to the wavelength) are present in the probed volume.

To conclude, the presented method shows good potential for quantitative three-dimensional imaging of optically dense, complex and inhomogeneous media, where errors arising from scattering and extinction ordinarily degrade the measurement accuracy. Compared to other experimental solutions also capable of diminishing the scattered light for line-of-sight detection, such as Ballistic imaging [2] and X-ray imaging [10, 11], the current technique suppresses this undesired intensity contribution *after* image acquisition, limiting it to less optically dense media. However, the method is compatible with other filtering approaches, such as temporal-, spatial- and polarization filtering (as utilized for Ballistic imaging), which could increase the range of applicability even further. Another benefit with the presented method concerns its relatively low experimental cost, the technique can for instance be used to study non-luminescent, optically dense objects running in steady-state operation using a simple CW laser combined with an inexpensive non-gated camera.

Acknowledgments

Finally, the authors wish to show their appreciation to the Linné Center within the Lund Laser Center (LLC) as well as CECOST through SSF and STEM for financial support. Also the ERC Advanced Grant DALDECS is acknowledged.

#162357 - $15.00 USD Received 1 Feb 2012; revised 29 Mar 2012; accepted 11 Apr 2012; published 13 Jun 2012